SCIENCE CHINA
Physics, Mechanics & Astronomy

• Article •

June 2013 Vol.56 No.6: 1079–1084
doi: 10.1007/s11433-013-5089-2

Controllable tune of the cutoff frequencies in a photonic crystal waveguide with hexagonal lattice

ZHU KongTao, DENG TianSong, SUN Yan, ZHANG QiFeng & WU JinLei*

Key Laboratory for the Physics and Chemistry of Nanodevices, Department of Electronics, Peking University, Beijing 100871, China

Received October 7, 2012; accepted November 7, 2012; published online May 3, 2013

In this paper, configuration parameters of the waveguide are altered independently or simultaneously to control the cutoff frequencies of the guided band. The independent control range of the upper and lower cutoff frequencies is 55.0% and 63.9% of the photonic band gap (PBG), respectively. The regulating range of the simultaneous tuning can be as large as 28.6% in terms of the PBG, or 240% in terms of the bandwidth. This tuning cutoff frequency method provides an efficient way to tailor the guided band and further tune the optical properties of PhCWs.

photonic crystal, waveguide, cutoff frequency, coupled mode, controllable tune

PACS number(s): 41.20.Jb, 42.25.Bs, 42.68.Ay, 42.82.Et, 92.60.Ta

Citation: Zhu K T, Deng T S, Sun Y, et al. Controllable tune of the cutoff frequencies in a photonic crystal waveguide with hexagonal lattice. Sci China-Phys Mech Astron, 2013, 56: 1079–1084, doi: 10.1007/s11433-013-5089-2

1 Introduction

Photonic crystals (PhCs) has been a focus of research interest because of photonic band gaps (PBGs), which can prohibit light in particular frequencies in crystals [1–6]. By introducing defects into a perfect PhC, different types of optical devices can be designed for different purposes [7–11]. In particular, PhCs with a line defect are called PhCWs, have revealed excellent properties in controlling light. Specifically, the fine tuning of the band edges of the light propagating in the PhCW makes it unique in optical structure design.

Because of the line defect, a guided band will likely emerge in PBG. Different types of line defect structures make the dispersion relations of the guided band various, and allow the PhCW to show different optical properties [12–18]. Specifically, the dispersion relation of the guided band determines not only the pass band range of the waveguide, but also affects the group velocities of the guided modes. There are various methods to tune the band edges. The methods can be divided into two types. One is to tune the dielectric constant of the material or the background. Most post-processing tuning methods are contained in this type [19]. Limited to the dielectric constant of the materials, this method cannot realize the fine tuning of the band edges. The other is to tune the radii or positions of the rods in the defect row or the rods in the first or the second row adjacent to the defect row. This method can tune the band edges precisely and effectively. Although a great many integrated optical devices based on PhCWs have been investigated [20–23], the study on finding an effective way to control the cutoff frequency is rare and the changing steps of the parameters to control the cutoff frequencies are only 1/1000 of the lattice constant (only about 1 nm), which is hard to realize in practical fabrication methodology [24,25].

In this paper, we propose a relatively effective method, which is of the second type, to control the upper and lower cutoff frequencies accurately. Three structural parameters are chosen to tune the cutoff frequencies, and the changing

*Corresponding author (email: jlwu@pku.edu.cn)

© Science China Press and Springer-Verlag Berlin Heidelberg 2013

steps of the parameters are set to 0.02a (about 10 nm in our model, a is the lattice constant equaling 500 nm). This dimension can be realized in practical fabrications. The band diagram of a two-dimensional (2D) PhCW with hexagonal lattice is calculated with the plane wave expansion method (PWEM). Then the influence of the parameters on the upper and lower cutoff frequencies of the guided band is systematically investigated. The method to control them independently and simultaneously is also presented.

2 The influence of three parameters on the cutoff frequencies

The simulated model is shown in Figure 1(a). It is constructed with the infinite hexagonal lattice of rods, where every second rod of the two-rod-separations in the central row is removed. In our model, the dielectric constant ε = 11.56 (corresponding to Si in the infrared region) [26]. To obtain the largest gap-midgap ratio [27], the radius r is set to 0.18a. Using the Massachusetts Institute of Technology photonic-bands package (software using the PWEM), the simulated band diagram of this structure is shown in Figure 1(b). The supercell method is used to calculate the band structure in the calculations. If the supercell size is selected too small, the coupling between the adjacent parallel waveguides cannot be neglected and the the simulated results will not be precise enough. If the supercell size is selected too large, the calculated time will be rendered ineffective (increasing with the supercell size exponentially). Considering both the cases above, the supercell size is selected to be 2a×9a, which can both obtain a balance between the calculated time and precise results.

In the simulated band diagram, there is a single mode guided band in the PBG. The upper and lower cutoff frequencies of the guided modes are at 0.416 and 0.393, in regard to the normalized frequency $\omega a/2\pi c$. Here ω is the angular frequency, and c is the light velocity in vacuum.

In general, the upper and lower cutoff frequencies of the guided band are affected by the PhCW structural parameters. Three different structural parameters r_d, r_a (subscript d represents defect, subscript a represents adjacent) and y are chosen, and the influence of the parameters on the upper and lower cutoff frequencies are investigated. Here r_d represents the radius of the defect rods, r_a represents the radius of the rods adjacent to the defect row and y represents the position of the rods adjacent to the defect row as shown in Figure 2(a). We have found that the variations of the cutoff frequencies with r_a, r_d and y are compelling.

Firstly, with a constant r_a and a constant y, both the upper and lower cutoff frequencies are decreased as r_d is increased. Suppose, r_a = 0.18a, y = 1.00a and r_d is increased from 0.10a to 0.18a, the upper cutoff frequency of the guided band is decreased from 0.440 to 0.416, while the lower cutoff frequency is decreased from 0.398 to 0.393 as shown in Figure 2(b). The upper cutoff frequency is decreased about five times faster than the lower one. To explain this phenomenon, we need to analyze the effects made by the increasing of r_d. When r_d is increased, the effective dielectric constant of the waveguide is also increased. As a result, the guided band is pulled down into the dielectric band [28]. At the same time, the propagation of the waveguide depends on the coupling between the defect modes of the cavities in the PhCW. The bandwidth of the guided band implies the coupling strength, which indicates that a wider bandwidth of the guided band reveals a stronger coupling between the cavities, and vice versa. When r_d is increased, each cavity is compressed and the coupling between the cavities is weakened. The bandwidth of the guided band is narrowed consequently [29]. As the two reasons analyzed above, the upper cutoff frequency is decreased faster than the lower one.

Secondly, with a constant r_d, a constant y, the calculated

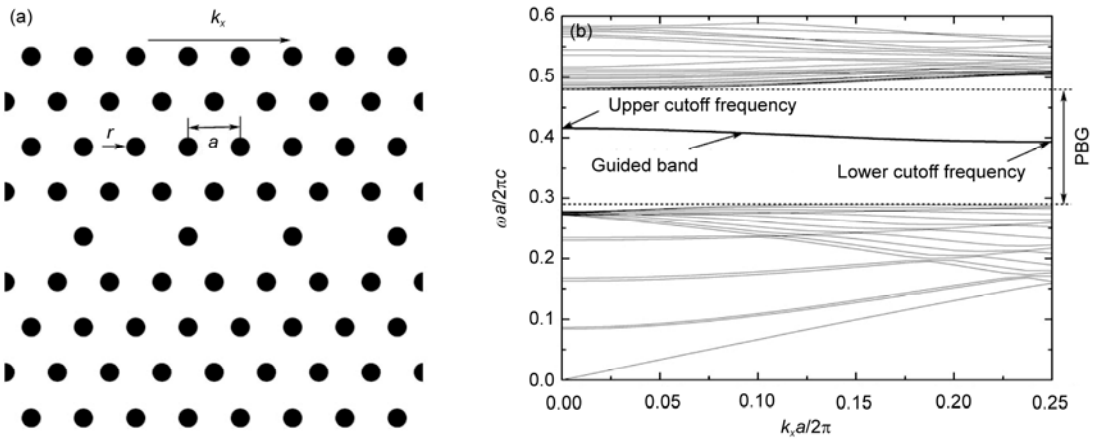

Figure 1 (a) Infinite hexagonal lattice of dielectric cylinders, in which every second rod of the two-rod-separations in the central row is removed. Dielectric constant ε = 11.56 and radii r = 0.18a, where a is the lattice constant. k_x represents the wave vector along the propagation direction. (b) Band diagram of the TM guided modes (the direction of the electric field is in parallel with the dielectric cylinders) in a PhCW. Thick line represents the dispersion relation of the guided band in the waveguide.

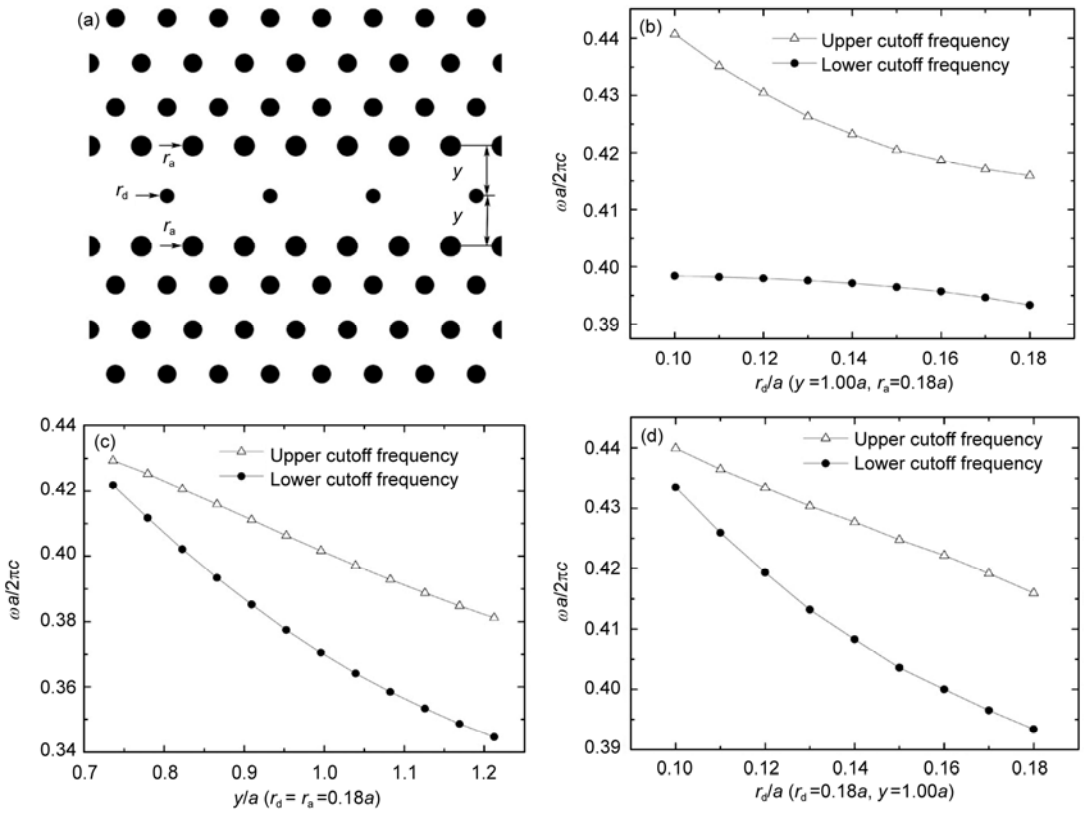

Figure 2 (a) Three parameters are selected to control the two cutoff frequencies. r_d represents the radius of the defect rods, r_a represents the radius of the rods adjacent to the defect row and y represents the position of the rods adjacent to the defect row. To illuminate the parameters clearly, we set r_a, r_d and y as follows: $r_a = 0.20a$, $r_d = 0.14a$, $y = 1.00a$. (b) Variations of the two cutoff frequencies with r_d. (c) Variations of the two cutoff frequencies with y. (d) Variations of the two cutoff frequencies with r_a.

results show that both the upper and lower cutoff frequencies are decreased as r_a is increased. Specifically, if $r_d = 0.18a$, $y = 1.00a$ and r_a is increased from $0.10a$ to $0.18a$, the upper cutoff frequency of the guided band is decreased from 0.440 to 0.416, while the lower cutoff frequency is decreased from 0.434 to 0.393 as shown in Figure 2(d). In the simulation, the lower cutoff frequency is decreased about twice as fast as the upper one, which indicates that the guided band is pulled down and broadened. We can also explain this phenomenon from two view points. The increasing of r_a makes the effective dielectric constant larger, thus pulls down the guided band into the dielectric band. Meanwhile, the increasing of r_a indicates a relative decreasing of r_d in the cavity. Therefore the coupling between the cavities is strengthened with the increasing of r_a. As a result, the guided band becomes broader and the upper cutoff frequency is decreased slower than the lower one.

Thirdly, with a constant r_a, a constant r_d, we find that both the upper and lower cutoff frequencies are decreased as y is increased. In particular, if $r_a = 0.18a$, $r_d = 0.18a$ and y is increased from $0.74a$ to $1.22a$, the upper cutoff frequency of the guided band is decreased from 0.429 to 0.381, while the lower cutoff frequency is decreased from 0.422 to 0.345 as shown in Figure 2(c). Here the lower cutoff frequency is decreased about twice as fast as the upper one. The coupled mode theory [29] can also be used to explain this phenomenon. With the increasing of y, the cavity size is enlarged and the coupling between the cavities is strengthened. Thus the guided band is broadened and the lower cutoff frequency is decreased about twice that of the upper one.

3 Independent control of the upper and lower cutoff frequencies

From the results above, it can be found that the upper cutoff frequency is susceptible to r_d and the lower cutoff frequency is susceptible to r_a and y. To further study the effects of the three parameters on the two cutoff frequencies, extensive calculations have been made. As mentioned above, the changing steps are set to $0.02a$. The variations of the three parameters r_a, r_d and y are from $0.10a$ to $0.30a$, from $0.10a$ to $0.30a$, from $0.44a$ to $1.30a$, respectively. It is found that if r_a, r_d and y are changed simultaneously, independent con-

trol of the upper and lower cutoff frequencies of the guided band can be realized as shown in Figures 3 and 4, respectively. From the extensive calculations, it is found that if y is increased and r_d is decreased, while r_a is altered slightly, the lower cutoff frequency is changed independently while the upper one is kept unchanged. By altering y from $0.72a$ to $1.04a$, r_d from $0.20a$ to $0.12a$ and r_a from $0.20a$ to $0.16a$, the lower cutoff frequency is decreased from 0.413 to 0.363, while the upper one is kept constant at 0.416. Conversely, if y is increased greatly, while r_d and r_a are decreased slightly, the upper cutoff frequency is changed independently while the lower one is kept unchanged. By changing r_d from $0.20a$ to $0.10a$, y from $0.86a$ to $1.04a$ and r_a from $0.20a$ to $0.14a$, the upper cutoff frequency is increased from 0.406 to 0.444, while the lower one is kept 0.383.

Also the largest ranges of the independent control of the upper and lower cutoff frequencies are investigated from the calculated data. As shown in Figure 5, the largest inde-

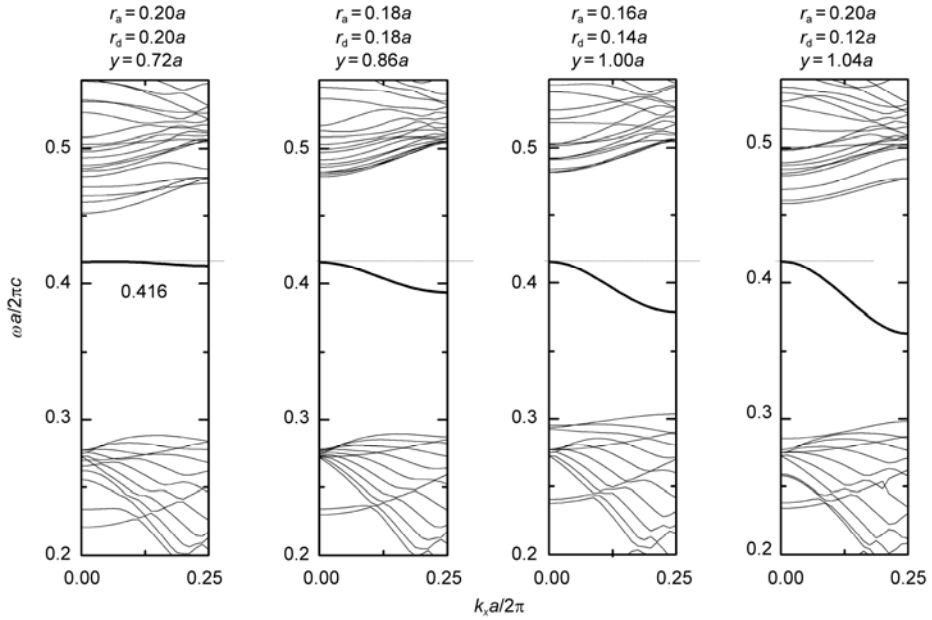

Figure 3 Independent control of the lower cutoff frequency. Thick lines represent the dispersion relations of the guided band with different lower cutoff frequencies and the conserved upper cutoff frequency.

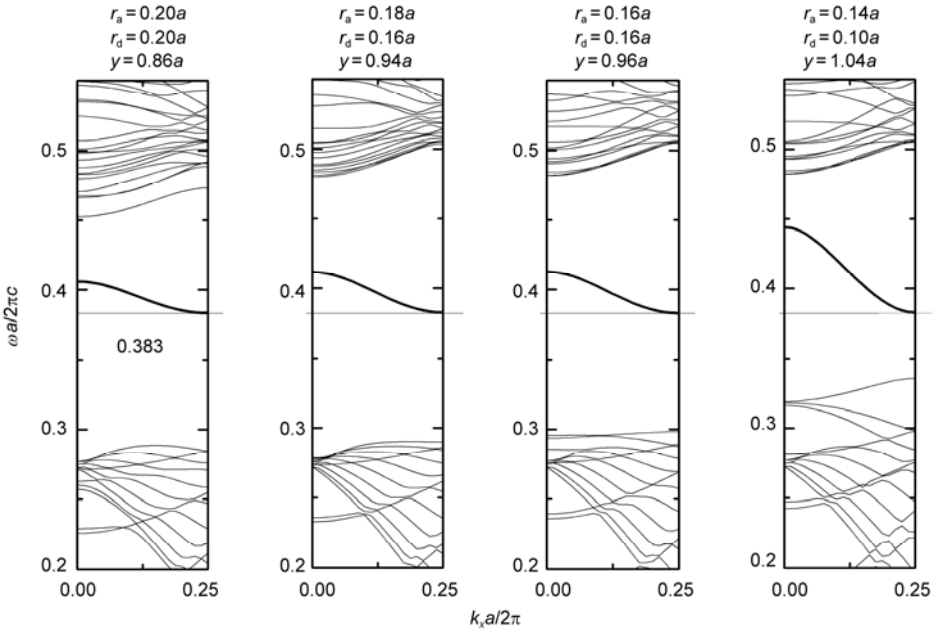

Figure 4 Independent control of the upper cutoff frequency. Thick lines represent the dispersion relations of the guided band with different upper cutoff frequencies and the conserved lower cutoff frequency.

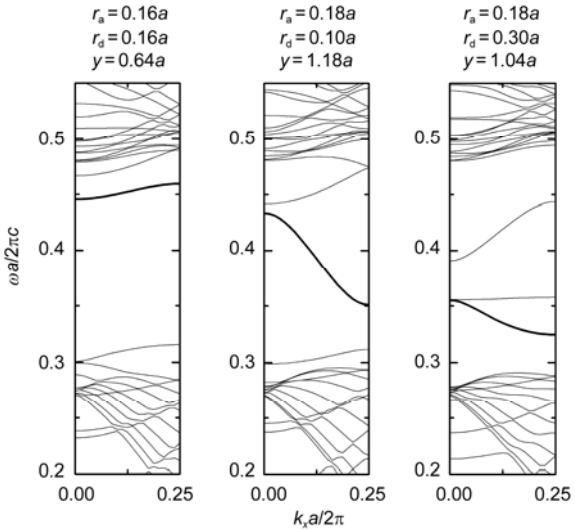

Figure 5 Ranges of the independent control of the cutoff frequencies. Thick lines represent the dispersion curves of the guided band. The left thick line shows the largest upper and lower cutoff frequencies. The middle thick line shows the largest bandwidth. The right thick line shows the lowest upper and lower cutoff frequencies.

pendent control range of the lower cutoff frequency is from 0.324 to 0.446. For the upper cutoff frequency, the largest independent control range is from 0.355 to 0.459. The largest regulating ranges for the lower and upper cutoff frequencies are 63.9% and 55.0% in terms of the frequency ranges of PBG, respectively.

4 Simultaneous control of the upper and lower cutoff frequencies

Furthermore, it is found that if r_a and r_d are altered with the same change with y being constant, the upper and lower cutoff frequencies can be tuned simultaneously. By altering r_a and r_d from $0.10a$ to $0.20a$ and y being $0.86a$, the frequency range of the guided band can be moved from 0.439–0.460 to 0.383–0.405, while the bandwidth is kept constant as shown in Figure 6. The two cutoff frequencies are decreased with the same distance, when r_a and r_d are increased with the same change. Using the coupled mode theory, this phenomenon can be explained qualitatively. When r_a and r_d are altered with the same changes, the coupling strength is kept unaltered. Therefore the bandwidth of the guided band is kept unchanged and the upper and lower cutoff frequencies are tuned simultaneously. The regulating range of the guided band can be as large as 28.6% in terms of the PBG, or 240% in terms of the bandwidth.

All the data above is based on our model, an infinite hexagonal lattice of rods. If the case is finite in the vertical direction, the band diagram and the guided band will differ. A light line will appear in the band diagram subsequently.

5 Conclusions

A method is proposed and demonstrated to accurately control the upper and lower cutoff frequencies of the guided band in a PhCW. It is shown that the two cutoff frequencies are relative to r_a, r_d and y in the PhCW. By changing the three parameters simultaneously, one cutoff frequency can be tuned independently while the other one is kept constant. The largest regulating independent ranges of the lower and upper cutoff frequencies are 63.9% and 55.0% in terms of the PBG, respectively. By changing r_a and r_d with the same extent, the two cutoff frequencies can be tuned simultaneously with the same distance. The regulating range of this simultaneous tune can be as large as 28.6% in terms of the PBG, or 240% in terms of the bandwidth. Using this tuning

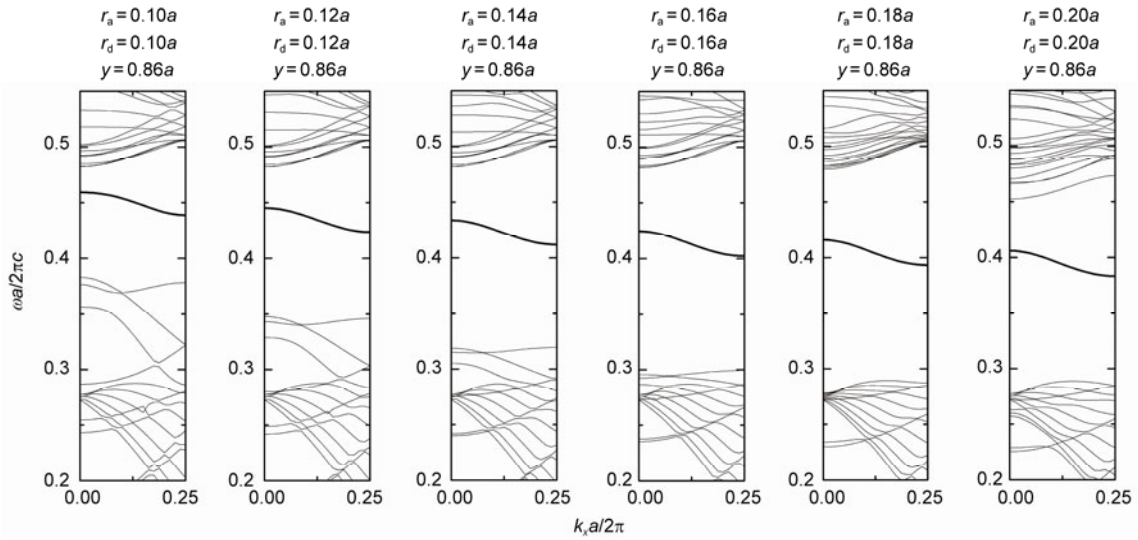

Figure 6 Simultaneous control of the two cutoff frequencies. Thick lines represent the dispersion curves of the guided band with the same bandwidth.

band dispersion method, the band edges and other optical properties can be further tuned in PhCW.

This work was supported by the Ministry of Science and Technology of China (Grant No. 2007CB936204) and the National Natural Science Foundation of China (Grant Nos. 61271050, 61076057 and 61171023).

1 Joannopoulos J D, Villeneuve P R, Fan S H. Photonic crystals putting a new twist on light. Nature, 1997, 386: 143–149
2 Foresi J S, Villeneuve P R, Ferrera J, et al. Photonic-bandgap microcavities in optical waveguides. Nature, 1997, 390: 143–145
3 Fan W L, Zhang X C, Dong L F. Two-dimensional plasma photonic crystals in dielectric barrier discharge. Phys Plasmas, 2010, 17: 113501–113507
4 Nair R V, Vijaya R. Photonic crystal sensors: An overview. Prog Quant Electron, 2010, 34: 89–134
5 Weiss S M, Rong G, Lawrie J L. Current status and outlook for silicon-based optical biosensors. Phys E, 2009, 41: 1071–1075
6 Beggs D M, O'Faolain L, Krauss T F. Accurate determination of hole sizes in photonic crystal slabs using an optical measurement. Phys E, 2009, 41: 1115–1117
7 Lin C Y, Wang X L, Chakravarty S, et al. Wideband group velocity independent coupling into slow light silicon photonic crystal waveguide. Appl Phys Lett, 2010, 97: 183302–183304
8 Hou J, Gao D S, Wu H M, et al. Flat band slow light in symmetric line defect photonic crystal waveguides. IEEE Photon Techno Lett, 2009, 21(20): 1571–1573
9 Vlasov Y A, O'Boyle M, Hamann H F, et al. Active control of slow light on a chip with photonic crystal waveguides. Nature, 2005, 438(3): 65–69
10 Geiss R, Diziain S, Iliew R, et al. Light propagation in a free-standing lithium niobate photonic crystal waveguide. Appl Phys Lett, 2010, 97: 131109–130011
11 Chen X N, Jiang W, Chen J Q, et al. 20 dB-enhanced coupling to slot photonic crystal waveguide using multimode interference coupler. Appl Phys Lett, 2007, 91: 091111–091113
12 Yan M B, Gong Q, Wang H L. Defect and dope selective of transmission properties of 2D photonic crystal. Optik, 2010, 121: 2133–2136
13 Baba T, Mori D. Slow light engineering in photonic crystals. J Phys D-Appl Phys, 2007, 40: 2659–2665
14 Baba T, Kawasaki T, Sasaki H, et al. Large delay-bandwidth product and tuning of slow light pulse in photonic crystal coupled waveguide. Opt Express, 2008, 16(12): 9245–9253
15 Dong G Y, Yang X L, Cai L Z. Transmission properties of an air waveguide with left-handed holographic photonic crystal cladding. Chin Phys Lett, 2011, 28(1): 014210–014213
16 Schulz S A, O'Faolain L, Beggs D M, et al. Dispersion engineered slow light in photonic crystals: A comparison. J Opt, 2010, 12: 104004–104013
17 Feng S, Chen X, Yang D, et al. Engineering the group velocities of the guiding modes in two-dimensional annular coupled-cavity waveguides. J Opt, 2011, 13: 015705–015709
18 Zhu K T, Deng T S, Sun Y, et al. Design of wideband and low dispersion based on coupled cavity waveguides. Opt Commun, 2012, 285: 2611–2614
19 Wu J, Li Y P, Peng C, et al. Numerical demonstration of slow light tuning in slotted photonic crystal waveguide using microfluidic infiltration. Opt Commun, 2011, 284: 2149–2152
20 Tsai Y L, Lan H C, Lin S F, et al. Design of low-loss tapered waveguide by applying photonic-crystal-based microlenses in telescopic structure. Opt Rev, 2010, 17(6): 536–540
21 Ferrier L, Daif O E, Letartre X, et al. Surface emitting microlaser based on 2D photonic crystal rod lattices. Opt Express, 2009, 17(12): 9780–9788
22 Gan L, Zhou C Z, Wang C, et al. Two-dimensional air-bridged silicon photonic crystal slab devices. Phys Status Solidi A, 2010, 207(12): 2715–2725
23 David A, Benisty H, Weisbuch C. Spontaneous emission in GaN InGaN photonic crystal nanopillars. Opt Express, 2007, 15(26): 17991–18004
24 Chen X Y, Shum P, Hu J J. Special control of the cutoff frequencies in a 2D photonic crystal coupled-cavity waveguide. Opt Commun, 2007, 276: 93–96
25 Yatsui T, Lim J, Nakamata T, et al. Low-temperature (~270°) growth of vertically aligned ZnO nanorods using photoinduced metal organic vapour phase epitaxy. Nanotechnology, 2007, 18: 065606–065609
26 Florescu M, Torquato S, Steinhardt P J. Effects of random link removal on the photonic band gaps of honeycomb networks. Appl Phys Lett, 2010, 97: 201103–201105
27 Jiang B, Liu A J, Chen W, et al. The optimization of large gap-midgap ratio photonic crystal with improved bisection-particle swarm optimization. Opt Commun, 2011, 284: 226–230
28 Joannopoulos J D, Johnson S G, Winn J N, et al. Photonic Crystals: Molding the Flow of Light. Princeton: Princeton University Press, 2008. 14–16
29 Ha S, Sukhorukov A A, Lavrinenko A V, et al. Cavity mode control in side-coupled periodic waveguides: Theory and experiment. Photonic Nanostruct, 2010, 8: 310–317